

Supporting information

**High-Performance Inverted Planar Heterojunction
Perovskite Solar Cells Based on Solution-Processed CuO_x
Hole Transport Layer**

Weihai Sun,^{a,b} Yunlong Li,^a Senyun Ye,^a Haixia Rao,^a WeiBo Yan,^a HaiTao Peng,^a

Yu Li,^b Zhiwei Liu,^{*a} Shufeng Wang,^b Zhijian Chen,^b Lixin Xiao,^b Zuqiang Bian^{*a}

and Chunhui Huang^a

^aBeijing National Laboratory for Molecular Sciences, State Key Laboratory of Rare Earth Materials Chemistry and Applications, Peking University, Beijing, 100871, P. R. China.

^bInstitute of Modern Optics and State Key Laboratory for Artificial Microstructure and Mesoscopic Physics, School of Physics, Peking University, Beijing 100871, P. R. China.

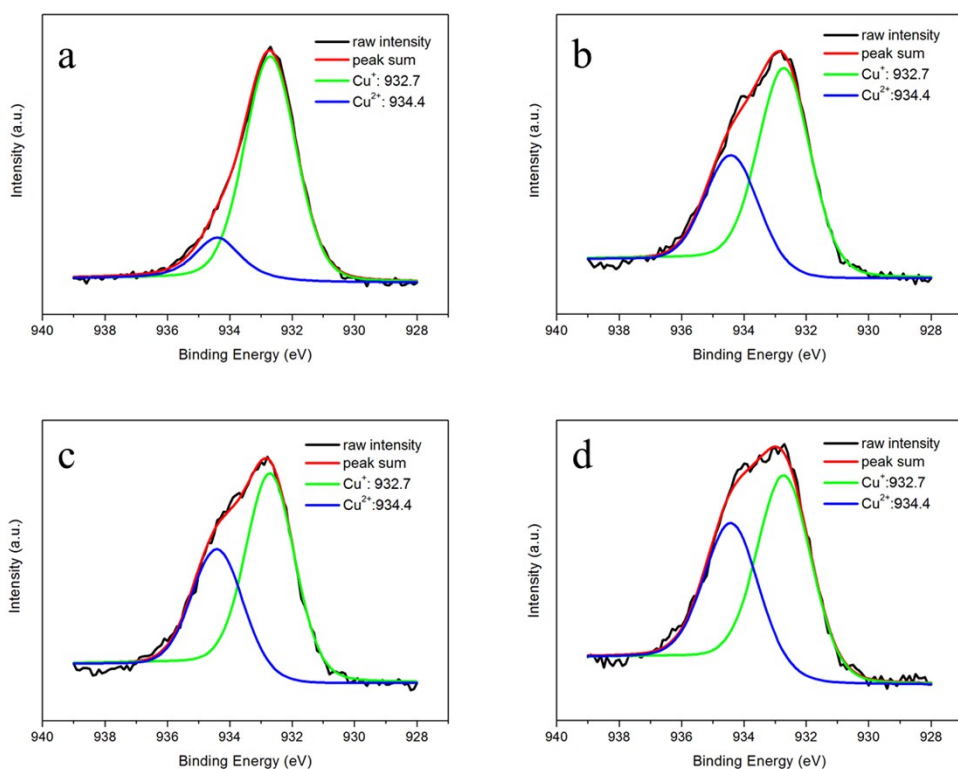


Fig. S1. XPS spectra of the Cu 2p_{3/2} peaks for CuO_x films fabricated from the different UV-O₃ treating times: 0 min (a), 15 min (b), 30 min (c), 60 min (d).

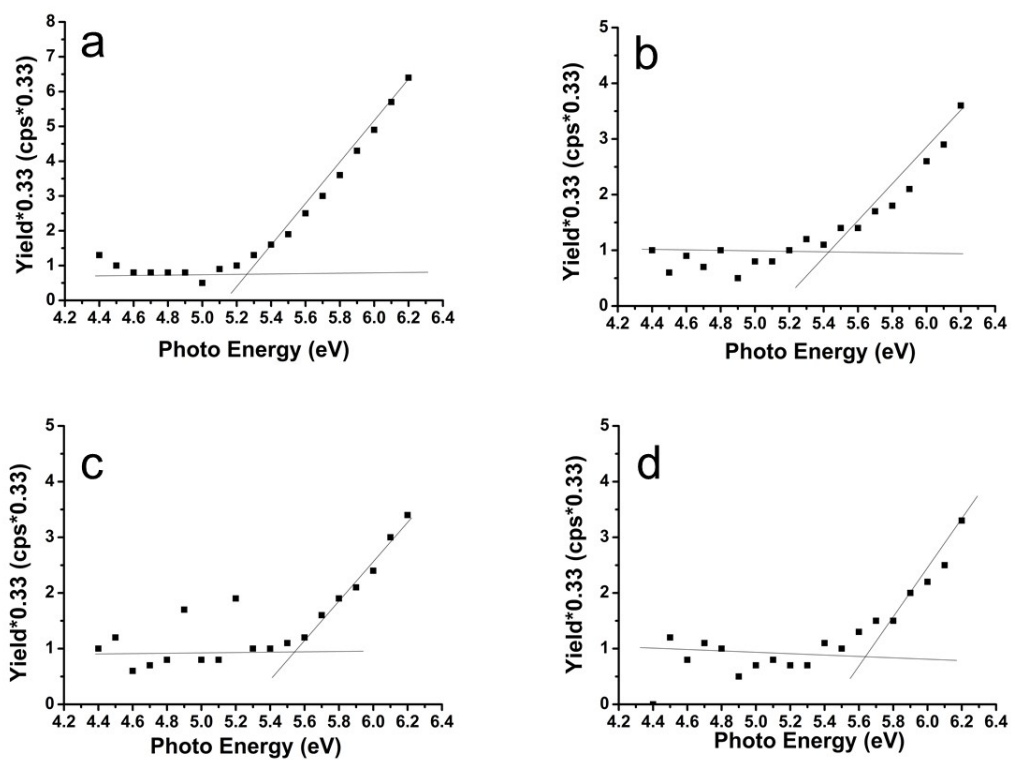


Fig. S2. The ultraviolet photoelectron yield spectroscopy of CuO_x films fabricated

from the different UV-O₃ treating times: 0 min (a), 15 min (b), 30 min (c), 60 min (d).

Table S1. The HOMO of CuO_x films fabricated under the different UV-O₃ treating times

The UV-O ₃ treating times (min)	0	15	30	60
HOMO (eV)	-5.2	-5.3	-5.5	-5.6

Table S2. The related PL data of the CH₃NH₃PbI₃ perovskite prepared at the top of different hole transport layers.

Hole transport layer	τ_1 (ns)	Fraction	τ_2 (ns)	Fraction
PEDOT:PSS	2.5	53.9	6.8	46.1
CuO _x	0.9	79.9	9.8	20.1

Comparison for two perovskite fabrication method. To deposit CH₃NH₃PbI₃, there are two available methods (the FDC and two-step coating methods) used in our device fabrication process. After being thermal treatment for 10 min, the C₆₀ (40 nm), BCP (8 nm) and Ag (100 nm) layers were sequentially deposited on the CH₃NH₃PbI₃ film by thermal evaporation inside a vacuum chamber (10⁻⁶ mbar). The current density-voltage (*J-V*) curves and corresponding photovoltaic parameters of the two devices, of which the perovskite layer deposited by the two-step coating method was noted as Device A while the perovskite layer deposited by the FDC method was noted as Device B, are shown in Fig. S3 and Table S3, respectively. As can be seen from the chart, Device A shows a PCE of 11.7%, a V_{oc} of 0.95 V, a J_{sc} of 20.6 mA/cm² and a FF of 59.9%. As expected, Device B exhibits a higher V_{oc} (0.99 V), J_{sc} (21.6 mA/cm²), FF (71.8%), producing a superior PCE of 15.3%. As previously reported¹, this can be attributed to a more dense and uniform perovskite film fabricated by the FDC method.

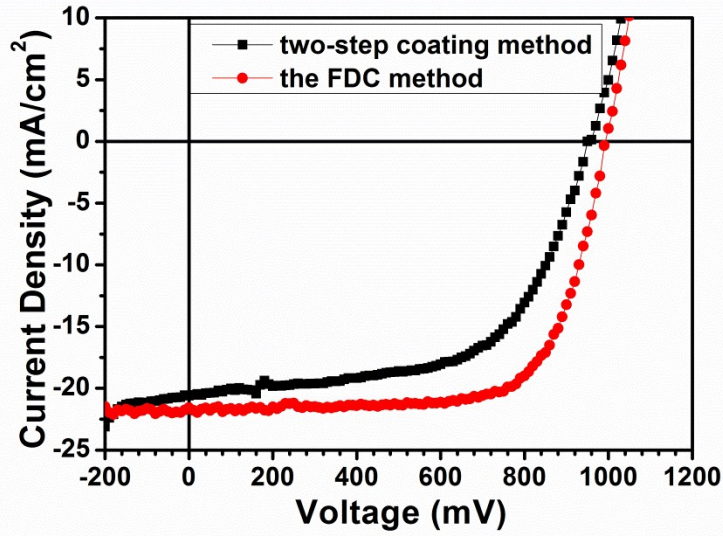


Fig. S3. The J - V curves of the perovskite solar cells with CuO_x films, where the perovskite layer fabricated by the two-step coating method and the FDC method.

Table S3. The photovoltaic parameters of perovskite solar cells with CuO_x hole transport layer (where the perovskite layer fabricated by the two-step coating method and the FDC method).

The perovskite fabricated method	V_{oc} (V)	J_{sc} (mA/cm ²)	FF (%)	PCE (%)
The two-step coating method	0.95	20.6	59.9	11.7
The FDC method	0.99	21.6	71.8	15.3

Optimization of the FDC method for perovskite solar cells. As we mentioned above, the quality of perovskite film have great effect on the photovoltaic performance of devices with CuO_x . Therefore, we have achieved the different morphologies (Figure S4) of perovskite film by adjusting the dropping time (3.5 s, 4.5 s, 5.5 s) of CB after introducing DMF solution of $\text{CH}_3\text{NH}_3\text{PbI}_3$ to the surface of CuO_x film. Furthermore, the J - V curves and relevant photovoltaic parameters of corresponding devices with a structure of $\text{ITO}/\text{CuO}_x/\text{CH}_3\text{NH}_3\text{PbI}_3/\text{C}_{60}/\text{BCP}/\text{Ag}$ fabricated (where the $\text{CH}_3\text{NH}_3\text{PbI}_3$ film were deposited when the dropping time of CB was 3.5 s, 4.5 s and 5.5 s, noted as

Device C, Device D and Device E, respectively), are shown in Fig. S5 and Table S4. We found that the PCE of device increases first and then decreases as the dropping time increases. It could be explained from Fig. S4a and S4b that the perovskite fabricated when the dropping time was controlled in 3.5 s shows the poor uniformity and the cracks of perovskite film would increase the possibility of the recombination of charge carriers in device, thus leading to an inferior PCE. When the dropping time was extended to 4.5 s, the maximum PCE of device was obtained due to the high quality perovskite film fabricated (Fig. S4c and S4d). However, the PCE of device slightly decreased as the dropping time was delayed to 5.5 s, which could be ascribed to the increased grain boundary density caused by the smaller perovskite grain (Fig. S4e and S4f).

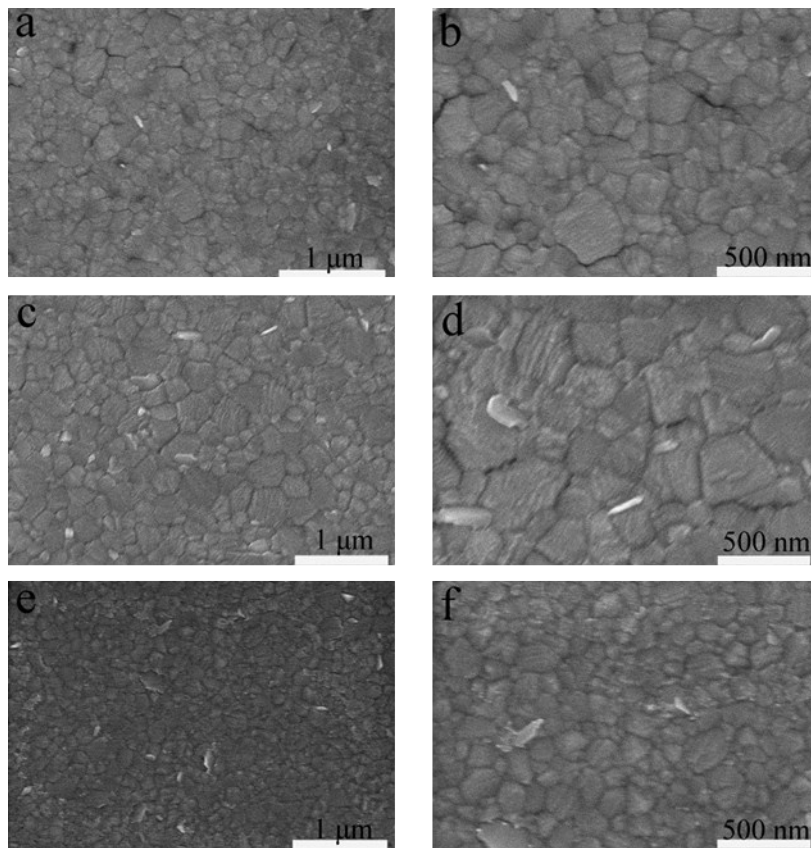


Fig. S4. SEM images of perovskite films fabricated by the FDC method under the different dropping time of the CB solution. a, b) 3.5 s; c, d) 4.5 s; e, f) 5.5 s.

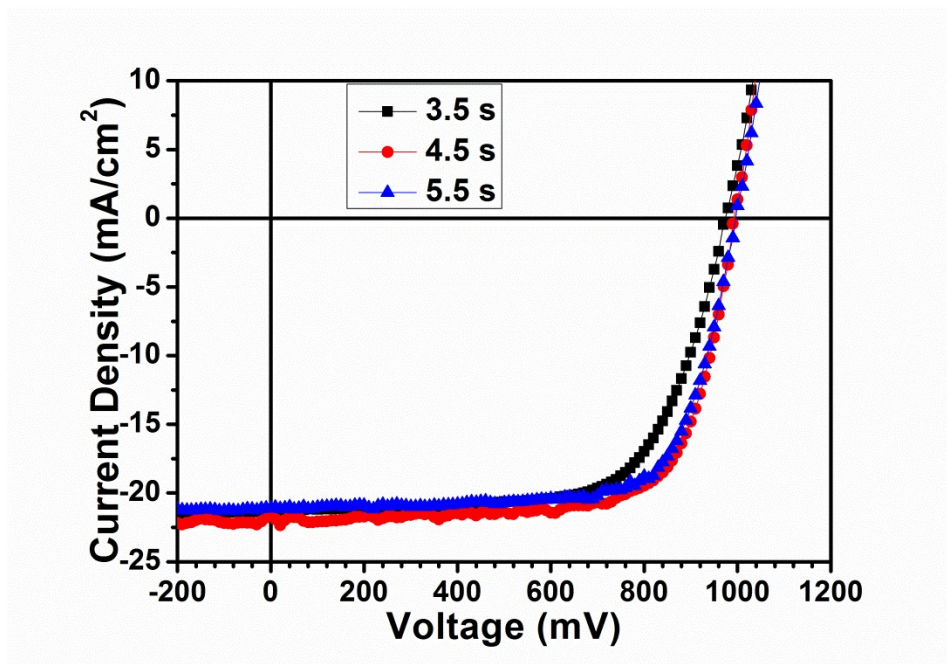


Fig. S5. The J - V curves of the perovskite solar cells with CuO_x films, where the perovskite layer fabricated by the FDC method under the different dropping time of the CB solution.

Table S4. The photovoltaic parameters of perovskite solar cells with CuO_x HTM, where the perovskite film prepared via adjusting the dropping time of the CB solution by the FDC method.

The dropping time of CB	V_{oc} (V)	J_{sc} (mA/cm ²)	FF (%)	PCE (%)
3.5 s	0.97	21.3	68.0	14.1
4.5 s	0.99	21.6	73.2	15.6
5.5 s	1.00	21.1	72.7	15.4

The influences of the ratio of $\text{Cu}^{2+}/\text{Cu}^+$ in CuO_x film on the performance of devices. A series of complete devices cooperated with CuO_x film under the different UV- O_3 treating times were assembled. Fig. S6 and Table S5 depicts the current density-voltage (J - V) curves of the perovskite solar cells employing different ratio of $\text{Cu}^{2+}/\text{Cu}^+$ in CuO_x film. It is interesting to note that all of our perovskite solar cells

present the similar PCE which maintain over 16%, indicating that the ratio of $\text{Cu}^{2+}/\text{Cu}^+$ in CuO_x film has little effects on the device performance. Meanwhile, the high PCE of device also reflect whether CuO or Cu_2O could form the ohmic contact between the ITO anode and the perovskite layer, thus accelerating the separation of holes from the interface layer and promoting the hole injection efficiency into ITO anode. However, the FF of device with CuO_x layer decreased slightly as the increased CuO in the hole transport layer, which are consistent with the previous literature results.

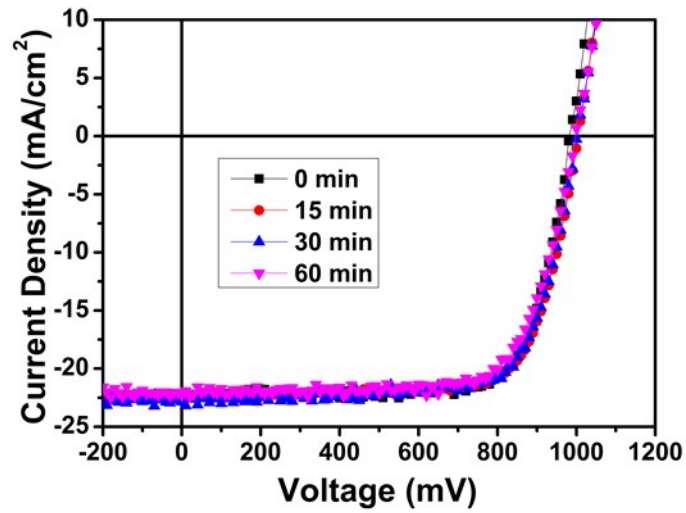


Fig. S6. The J - V curves of the perovskite solar cells with CuO_x films fabricated under the different UV- O_3 treating times.

Table S5. The photovoltaic parameters of perovskite solar cells with CuO_x HTM under the various UV-O₃ treating times.

UV-O ₃ treating times (min)	V_{oc} (V)	J_{sc} (mA/cm ²)	FF (%)	PCE (%)
0	0.98	22.3	77.0	16.8
15	1.00	22.3	74.8	16.7
30	1.00	22.8	73.8	16.9
60	1.00	22.3	72.1	16.1

Table S6. The photovoltaic parameters of perovskite solar cells with the different thickness of CuO_x layer.

The spin-coating speed (rpm)	Thickness (nm)	V_{oc} (V)	J_{sc} (mA/cm ²)	FF (%)	PCE (%)
3000	7	0.97	23.1	72.8	16.3
4000	5	0.97	23.4	75.3	17.1
5000	4	0.97	23.5	74.7	17.0
6000	3	0.97	23.2	73.7	16.6

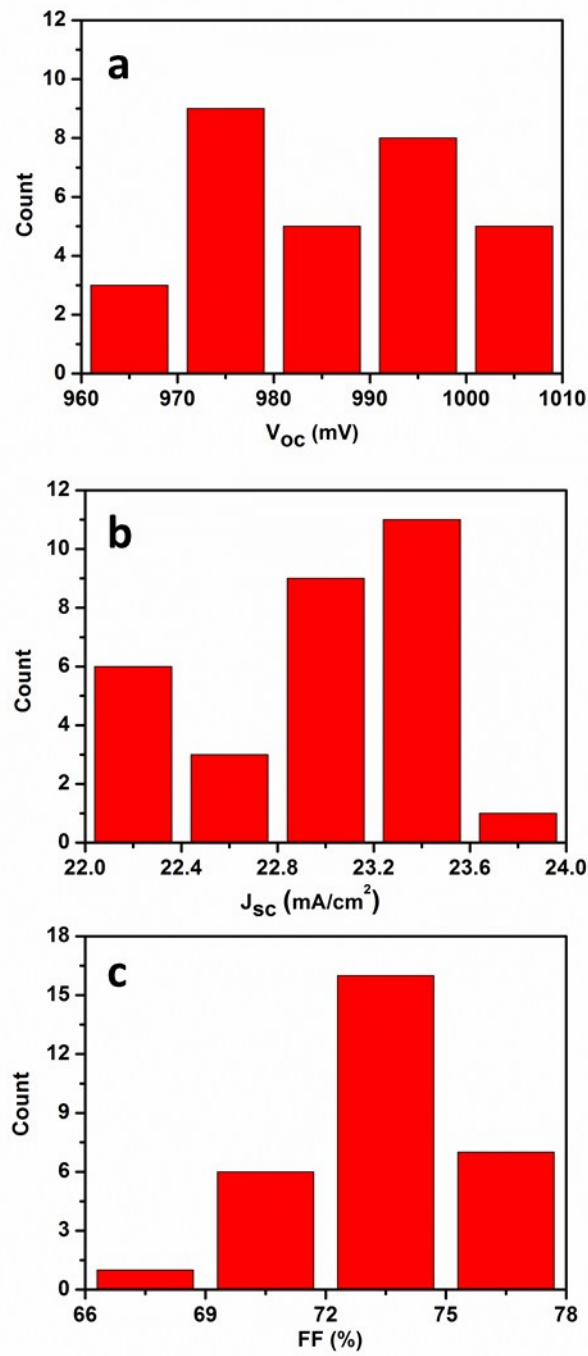


Fig. S7. The histograms of other performance parameters of V_{oc} , J_{sc} and FF for 30 independent perovskite solar cells fabricated with CuO_x hole transport layer.

Table S7. The photovoltaic parameters of perovskite solar cells with or without CuO_x layer (10 devices for each condition).

Hole transport layer	V_{oc} (V)	J_{sc} (mA/cm ²)	FF (%)	PCE (%)
None	0.91±0.01	21.5±0.2	61.5±1.0	12.1±0.1
CuO _x layer	0.98±0.01	23.1±0.3	73.9±1.2	16.7±0.2

1. S. Ye, W. Sun, Y. Li, W. Yan, H. Peng, Z. Bian, Z. Liu and C. Huang, *Nano Lett*, **2015**, 15, 3723.